AIAA JOURNAL
Vol. 31, No. 5, May 1993

Parameters Governing the Turbulent Wall Jet in an External Stream

M. D. Zhou* and I. Wygnanski†
University of Arizona, Tucson, Arizona 85721

Mean velocity distributions in a plane, turbulent, and fully developed wall jet embedded in a uniform stream were measured for a variety of initial velocity ratios and Reynolds numbers. It was determined that the bulk of the flow is self-similar, provided the maximum velocity in the jet is twice as large as the freestream velocity. The normalized velocity profile depends on two velocity scales and on two length scales that, in turn, depend on the momentum flux at the nozzle, the viscosity, and the initial velocity ratio between the jet and the freestream defined by $R \equiv (U_j - U_\infty)/(U_j + U_\infty)$. The width of the nozzle that was commonly used to reduce these data has no part in the similarity considerations. The approximate self-similarity may be used to estimate the skin friction that is otherwise determined with considerable difficulty.

Nomenclature

b = width of the slot
J = excess kinematic momentum flux near the nozzle, $\int_0^\infty (U - U_\infty)U \, dY \simeq U_j(U_j - U_\infty)b$
U = local velocity
U_j = jet velocity at the nozzle exit
U_m = local maximum velocity in the jet
U_∞ = freestream velocity
U_0 $\equiv (U_m - U_\infty)$
X = streamwise distance measured from the nozzle
Y = distance from the surface
Y_m = distance from the surface where the local velocity is maximum
$Y_{m/2}$ = distance from the surface where the local velocity is reduced to one-half of its maximum value $(Y_{m/2} > Y_m)$
Y_0 = outer length scale, identical to $(Y_{m/2} - Y_m)$
θ_0 $\equiv \{\int_0^\infty [1 - (U/U_\infty)](U/U_\infty) \, dY\}_{x=0}$
ν = kinematic viscosity of the fluid
ξ = dimensionless distance from the nozzle, $[XJ/\nu^2]$
ρ = density of the fluid
τ_w = shear stress at the wall

Introduction

WALL jets have many important applications in aeronautics. Not only does the flow over a cowl of a fan-jet engine or the flow over a film-cooled turbine blade belong to the wall-jet category, but the very concepts of boundary-layer control by blowing are based on this flow. Blowing from an external source is not a prerequisite to the generation of wall jets because they also occur on all lifting, slotted surfaces, slotted flaps being the prime examples. The quest for high-lift and therefore enhanced circulation is often associated with wall jets. Thus wall-jet flows may be found on airplane wings (F-104 Starfighter, A-6 Crusader) and more recently on helicopter tail booms (NOTAR). Consequently, there are hundreds of articles and reports associated with the wall jet and its potential applications.

Received Feb. 24, 1992; revision received Oct. 12, 1992; accepted for publication Oct. 14, 1992.

*Research Scientist, Department of Aerospace and Mechanical Engineering; also Professor of Aerodynamics, Nanjing Aeronautical Institute, People's Republic of China. Member AIAA.

†Professor, Department of Aerospace and Mechanical Engineering; also Lazarus Professor of Aerodynamics, Tel Aviv University, Tel Aviv, Israel. Member AIAA.

Wall jets may formally be regarded as boundary layers having a higher velocity near the surface than the prevailing velocity in the freestream. The plane wall jet, in the absence of an external stream, is a prototypical configuration whose characteristics have been investigated in great detail. Many of these investigations were critically reviewed by Launder and Rodi[1,2] in addition to a variety of other, more complex wall-jet configurations. The flow was traditionally scaled in a way that made its rate of spread and the decay of its maximum velocity in the direction of streaming dependent on the nozzle Reynolds number (e.g., Tailland and Mathieu[3]). The length scale used for scaling the flow was the nozzle dimension, whereas the velocity scale was the efflux velocity at the nozzle. Narasimha et al.[4] suggested that these length and velocity scales ought to be replaced by the initial momentum flux and the viscosity of the fluid for the wall jet in quiescent surroundings. Their suggestion was recently rediscovered[5] and found useful in eliminating the Re dependence of the local scales. It also enabled one to estimate τ_w from the momentum integral equation.

The scaling laws for the wall jet in a constant external stream are less obvious because of the absence of self-similarity.[6] Many investigators, however, assumed that the flow was approximately similar and continued to scale the relevant parameters of the flow by modifying them slightly to account for the finite velocity prevailing at large distances from the solid surface. Patel[7] was the first one to replace the slot width with the initial momentum thickness as the characteristic length scale. This suggestion is consistent with neglecting the frictional losses. Patel related the rate of spread of the flow to the velocity scale and to the freestream velocity by an empirical formula. Launder and Rodi[1] modified Patel's scaling by replacing the momentum thickness at the slot exit with the thickness determined from the local momentum flux, thus trading off the predictive value of Patel's scaling for an improved correlation with the data. The maximum velocity in the wall jet was related to the freestream velocity, in both articles, rather than to an initial momentum flux and to viscosity.[4] *Unfortunately, none of the suggested scales could collapse the data available from other experiments.*

The purpose of the present report is to review the scaling parameters of the wall jet in a uniformly moving stream and examine the limitation of the self-similarity assumptions. We focus our attention on the relatively novel scaling scheme used for the wall jet in the absence of an external stream and explore its extension to a blown boundary layer. These suggestions are backed by experiments carried out in air, in the absence of pressure gradient or surface curvature. The experimental techniques and apparatus are similar to those described in Ref. 5, except that the experiment was carried out in a wind tunnel. A schematic diagram of the nozzle geometry is shown in Fig.

Table 1 Test runs

No.	b, mm	U_j, m/s	U_∞, m/s	θ_0, mm	U_∞/U_j	R	$Re_j \times 10^{-3}$	Symbol
I	5.0	33.0	2.8	—	0.085	0.84	11	⊙
II	5.0	32.7	8.0	0.73	0.24	0.61	11	▽
III	5.0	33.0	12.5	0.72	0.38	0.45	11	⊡
IV	5.0	32.8	19.5	0.74	0.59	0.25	11	◇
V	5.0	20.5	5.05	0.99	0.24	0.60	7	▼
VI	5.0	20.8	8.0	0.73	0.38	0.44	7	■
VII	5.0	20.9	12.6	0.72	0.59	0.25	7	◆
VIII	5.0	21.0	19.5	0.74	0.93	0.037	7	+
IX	3.2	33.0	8.0	0.73	0.24	0.61	7	⌓
X	5.0	55.0	5.0	0.99	0.09	0.83	18	⬠
XI	5.0	33.0	8.0	8.61	0.24	0.61	11	✡
XII	5.0	33.0	12.0	8.52	0.38	0.47	11	✸

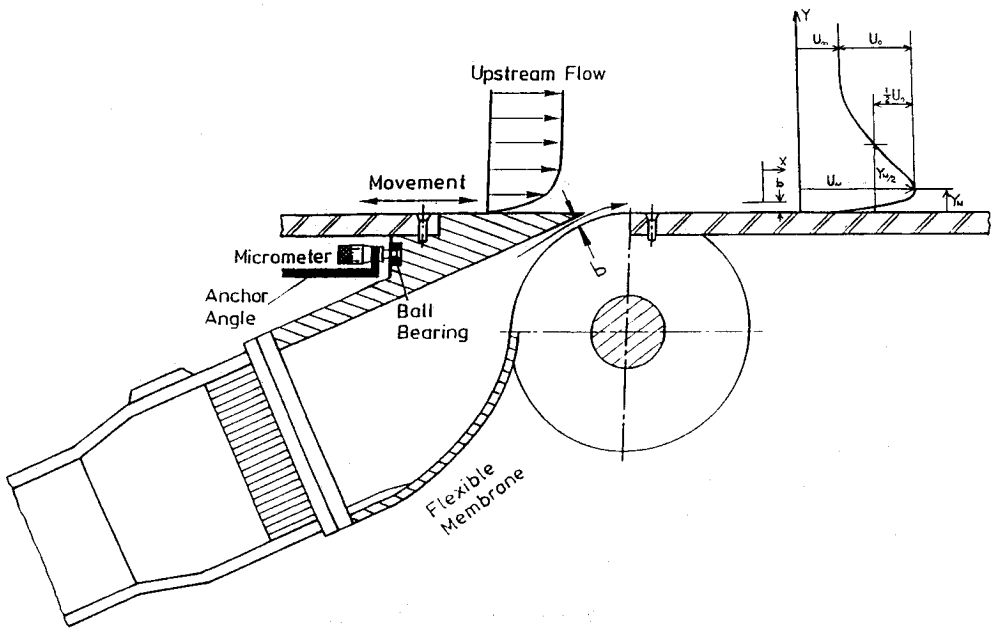

Fig. 1 Schematic diagram of the apparatus.

1. The flow was isothermal and incompressible, and the Reynolds numbers based on the jet efflux velocity and on the nozzle dimension ranged from approximately 7×10^3 to 1.8×10^4. Although the ratio between the freestream velocity and the jet velocity was allowed to vary from zero to unity, we shall concentrate on the fairly strong wall jet in which $U_\infty/U_m \leq 0.5$.

Summary of the Experimental Results

The streamwise component of the velocity was mostly measured in the developed and approximately self-similar region of the wall jet starting from 20 slot widths downstream of the nozzle and extending sometimes beyond 200 slot widths. The Reynolds number at the nozzle was altered by changing the efflux velocity and slot width. The ratio between the freestream velocity and the jet efflux velocity was also altered by varying U_∞ and U_j independently. The momentum thickness of the upstream boundary layer was calculated from velocity measurements made near the slot in the absence of the jet. Twelve sets of data listed in Table 1 were taken. Each set represents a data point in the independent parameter space.

The jet efflux velocity in sets I–IV, IX, XI, and XII was approximately 33 m/s, and in sets V–VIII it was 21 m/s, whereas the freestream velocity was altered. Three couples of sets (i.e., II and VI, III and VII, and IV and VIII) had the same freestream velocity and slot width but a different U_j. Thus sets II, V, IX, and XI and sets III, VI, and XII, as well as sets IV and VII, had the same ratio of U_∞/U_j while having different jet momentum and jet Reynolds number. The primary integral parameters characterizing the mean flow are sketched in Fig. 1. The streamwise variation of these parameters is significant, provided the normalized mean velocity profiles are self-similar. The extent to which self-similarity applies is discussed.

Discussion of Results

Some General Experimental Observations

Typical mean velocity profiles are plotted in dimensional form in Fig. 2 for the purpose of delineating the various stages in the development of the wall jet in the direction of streaming. Four sets of data are presented with progressively increasing effects of the upstream boundary layer from top to bottom. The top data set corresponds to $U_\infty/U_j = 0.085$, followed by 0.59, then 0.38, and finally 0.93. The slot width was maintained constant throughout ($b = 5$ mm). The momentum thickness of the upstream boundary layer was less than 1 mm in all but the third row, whereupon the value of θ_0 was artificially increased to 8.5 mm. *These data represent three distinctly different stages in the evolution of the wall jet in an external stream.* The velocity profiles in the top data set resemble the wall jet in the absence of an external stream at all X locations, and they contain only one inflection point in their outer region. Remnants of the upstream boundary layer persist over an increasing streamwise distance as one proceeds downward. The upstream boundary layer provides an additional inflection point in the outer region of the wall jet, and the effect of its relative thickness may be seen by comparing rows 2 and 3. A relatively strong U_j overcomes the velocity defect, whereupon a location is reached where the classical wall-jet profile emerges. The effect of the upstream boundary layer is much stronger in the bottom set, which resembles the development

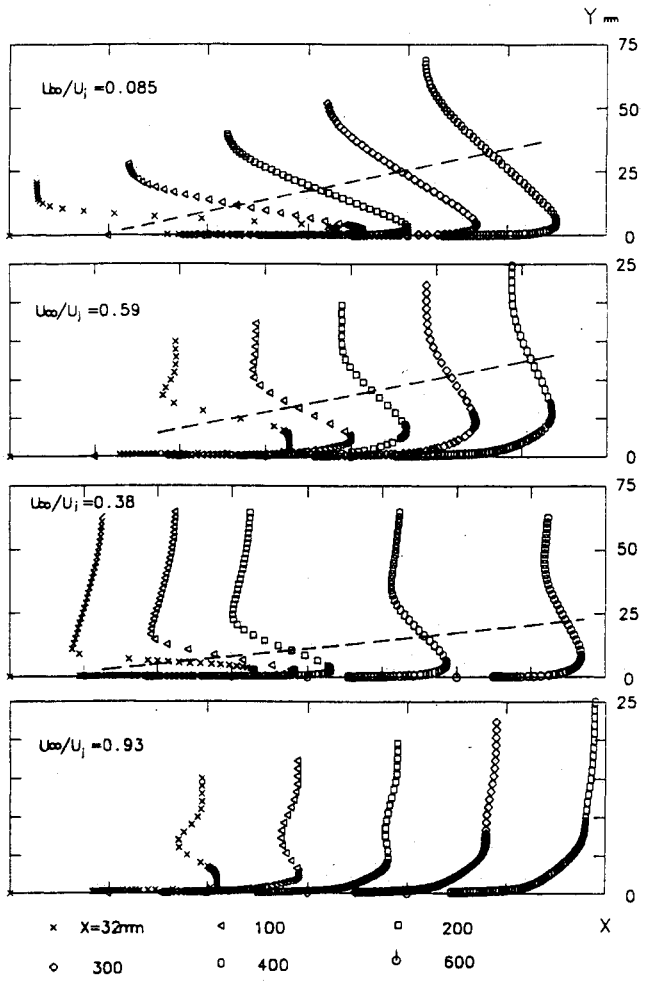

Fig. 2 Typical velocity distributions.

of a wake in the vicinity of a solid surface. Since the ratio of the freestream velocity to the jet velocity approaches unity near the nozzle, the flow appears to relax directly to an ordinary boundary layer without passing through the intermediate stage resembling the classical wall jet.

The local width of the wall jet, which is traditionally defined as the larger (outer) distance measured from the surface where the quantity $[(U-U_\infty)/(U_m-U_\infty)]=½$ and marked on Fig. 2 by dashed lines, is dominated by the velocity ratio while being hardly dependent on the relative thickness of the upstream boundary layer. At $X/b=100$, $Y_{m/2}\simeq 39$ mm for $U_\infty/U_j=0.085$, 20 mm for $U_\infty/U_j=0.38$, and only 14 mm for $U_\infty/U_j=0.59$ in spite of the fact that the upstream boundary layer disappears earlier in this case than in the row below it where the upstream boundary layer was artificially thickened.

The data presented and discussed in this manuscript exclude the effects of the upstream boundary layer on the normalized shape of the velocity profile. It is therefore concerned with those velocity ratios, U_∞/U_j, those X/b, and θ_0/b where the upstream boundary layer no longer affects the local shape of the mean velocity profile. The very weak blowing case, shown at the bottom of Fig. 2, is completely excluded.

Similarity of the Velocity Profiles

It is well known that a precise similarity of this flow is impossible.[6] The wall region may not be similar even in the absence of an external stream.[5] Nevertheless, many investigators managed to collapse some of their data on self-similar plots. The local velocity scale in the outer region of the wall jet should be $U_0\equiv(U_m-U_\infty)$, and the local dimensionless velocity in this region may be expressed by $(U-U_\infty)/U_0$. The no-slip condition at the wall imposes another velocity scale U_m on the inner boundary layer where the local U might be smaller than U_∞. Thus the wall jet in a uniform stream possesses two velocity scales: U_0 and U_m.

Plotting $(U-U_\infty)/U_0$ in the outer region and U/U_m in the inner region against a dimensionless distance from the wall $(Y/Y_{m/2})$ collapses the mean velocity profiles *measured in each data set* onto a single curve (Fig. 3). The collapse of the data is good, provided $U_\infty/U_m\leq 0.5$, a criterion that was not met when $U_\infty/U_j=0.59$ (i.e., for data sets IV and VII). The shape of the normalized mean velocity profile was affected by the ratio U_∞/U_j but was independent of Re_j on the scale shown, at least over the range of the Reynolds numbers considered in the present experiment. The normalized distance from the wall at which the velocity has attained its maximum value $Y_m/Y_{m/2}$ increased from 0.16 when $U_\infty\to 0$ to approximately 0.5 when $U_\infty/U_j=0.59$.

The rate of spread of $Y_{m/2}$ is greatly affected by the velocity ratio as is the virtual origin of the flow (Fig. 4a). All open symbols in this figure correspond to $Re_j=1.1\times 10^4$, whereas the darkened symbols represent $Re_j=7\times 10^3$, with the $\times$ symbols being the only exception corresponding to $Re_j=1.8\times 10^4$. Therefore, the differences in the rate of spread and in the virtual origin of the data measured at the same Re_j are attributed to changes in the velocity ratio. The influence of Re_j on $Y_{m/2}$ is almost as significant as of U_∞/U_j, particularly when U_∞/U_j is small (see the data representing $U_\infty/U_j=0.085$ and 0.24 in Fig. 4a).

The distance from the surface at which the velocity in the wall jet attains a local maximum (i.e., Y_m) is also an important parameter of the flow. The exact determination of Y_m is difficult from the raw data, which explains the relatively large scatter observed in Fig. 4b. Nevertheless, changing the ratio of U_∞/U_j and/or Re_j has no significant effect on the thickness of the inner flow, which increases linearly with X at a rate $dY_m/dX=0.0114$. The virtual origin of Y_m, which presumably depends on the shape of the nozzle and on the contraction ratio, is approximately $0.2b$. This quantity was subtracted from all local values of Y_m so that the line representing the data will pass through the origin irrespective of the slot width. Since the normalized velocity profiles are similar provided $U_\infty/U_m\leq 0.5$, the ratio of $(Y_m/Y_{m/2})$ should be independent of X but sensitive to U_∞/U_j. The dependence of $(Y_m/Y_{m/2})$ on U_∞/U_j increases rapidly at high values of U_∞/U_j, as marked on Fig. 3.

The strong dependence of $Y_{m/2}$ on U_∞/U_j and the concomitant independence of Y_m from this parameter suggest that the inner portion of the wall jet not only has its own velocity scale U_m but also its characteristic length scale Y_m. The characteristic width of the outer flow should be $Y_0\equiv(Y_{m/2}-Y_m)$. Using the different velocity and length scales for the inner and outer regions of the flow enabled us to collapse four out of the five groups of profiles plotted in Fig. 3 onto a single curve (Fig. 5a). The exclusion of the data corresponding to $U_\infty/U_j=0.59$ implies that this correlation should be limited to $0\leq(U_\infty/U_m)\leq 0.5$. This is a more stringent requirement than setting the independent parameter $U_\infty/U_j\leq 0.5$ because the quotient U_∞/U_m will always exceed 0.5 at large distances from the nozzle. The choice of $U_\infty/U_m=0.5$ is based on experimental observations, but the self-similar approximation does not instantly fail when this threshold value is exceeded. The self-similar profiles plotted in Fig. 5a are not more scattered than the velocity profiles plotted in the absence of an external stream that are also plotted in this figure. Enlarging the scale of the inner region (Fig. 5b) supports the use of the two parameter scalings chosen. The similarity in the inner region is not perfect, and one may discern a dependence on X as well as on Re_j. The dependence on X is more apparent in the immediate vicinity of the wall (Fig. 5c); however, it is diminished by the presence of the external stream (compare with Fig. 7 in Ref. 5). The task at hand is to determine uniquely the dependence of U_m, U_0, Y_m, Y_0, and, it is hoped, the skin friction τ_w on the independent variables governing this flow.

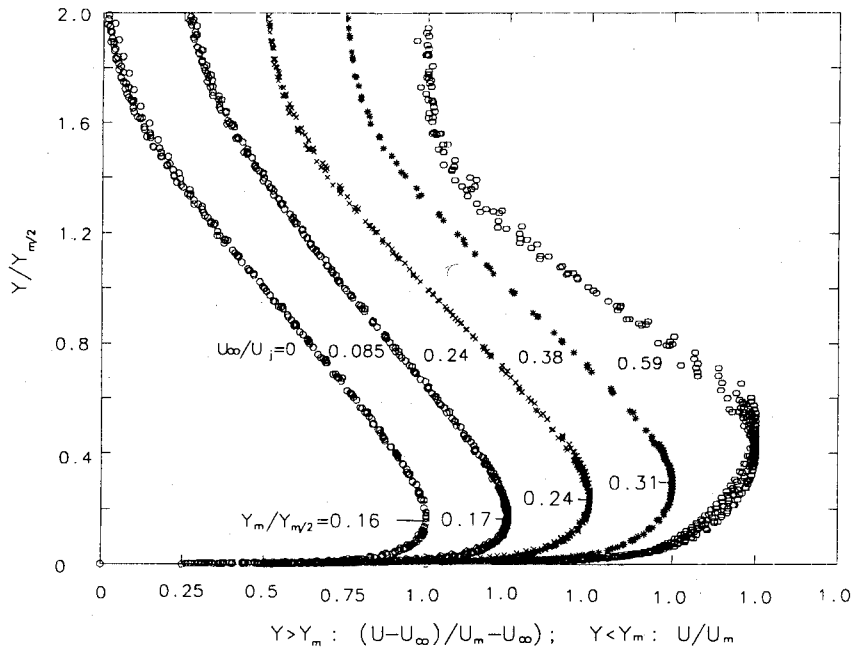

Fig. 3 Conventionally normalized mean velocity profiles.

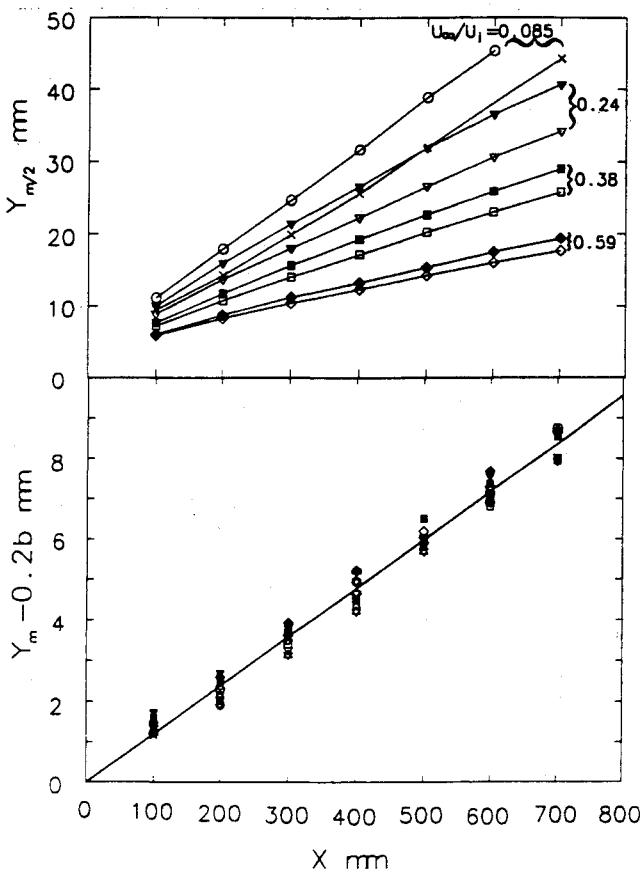

Fig. 4 Rate of spread of $Y_{m/2}$ and Y_m with X for various velocity ratios and Reynolds numbers.

Parameters Scaling the Flow

Narasimha et al.[4] suggested that the fully developed wall jet in the absence of an external stream should attain a local equilibrium independent of the detailed conditions at the nozzle. The sole parameter determining the evolution of such incompressible flow in a fluid of a given viscosity is its initial kinematic momentum flux. This approach correctly scaled the three most important parameters in the wall jet (i.e., $Y_{m/2}$, U_m, and τ_w), making them independent of Re_j and facilitating the evaluation of τ_w from the mean momentum equation.[5] The addition of the external stream suggests that *the parameter governing the flow is the excess of kinematic momentum flux near the nozzle,* which may have a simple form whenever the jet velocity is tangential to the freestream and is uniform:

$$J = \int_0^\infty (U - U_\infty)U \, dY = b(U_j - U_\infty)U_j - U_\infty^2\theta_0 \qquad (1)$$

A local momentum flux (measured at any streamwise location of interest) enables one to define a local θ used to collapse some wall jet data,[1] but this introduces additional empiricism and neglects the loss of momentum to skin friction.

In most laboratory experiments reported, the momentum deficit in the upstream boundary layer is negligible in comparison with the excess momentum flux of the jet. Thus, neglecting the last term on the right-hand side of Eq. (1) defines a dimensionless streamwise distance ξ:

$$\xi = \left[\frac{XJ}{\nu^2}\right] = \left[\frac{Xb(U_j - U_\infty)U_j}{\nu^2}\right] \qquad (2)$$

The utility of ξ depends on its ability to describe the streamwise evolution of all of the length and velocity scales, used in Fig. 5, uniquely. It is clear that two independent parameters are required to define ξ: the jet momentum bU_j^2 and the freestream velocity U_∞. It is not a priori obvious how the dependent parameters (U_m, U_0, Y_m, Y_0, and τ_w) relate to ξ and U_∞/U_j. In an attempt to separate the effect of Re from the effect of velocity ratio, we first plotted $(Y_{m/2} - 0.7b)J/\nu^2$ vs ξ and eliminated the effect of Re_j from the data plotted in Fig. 4. We subtracted $0.7b$ from all $Y_{m/2}$ values plotted in Fig. 4 to account for the initial width of the flow at $X \to 0$. The factor of 0.7 stems from replacing the top-hat velocity profile existing at the nozzle with a fictitious wall-jet profile at $\xi = 0$. The dependence of $(Y_{m/2} - 0.7b)J/\nu^2$ on U_∞/U_j remained virtually unchanged (Fig. 6a).

We then defined a dimensionless velocity ratio parameter:

$$R \equiv (U_j - U_\infty)/(U_j + U_\infty) \qquad (3)$$

and used it to divide the data plotted in Fig. 6a and collapse it onto a single curve (Fig. 6b); R was chosen initially because of

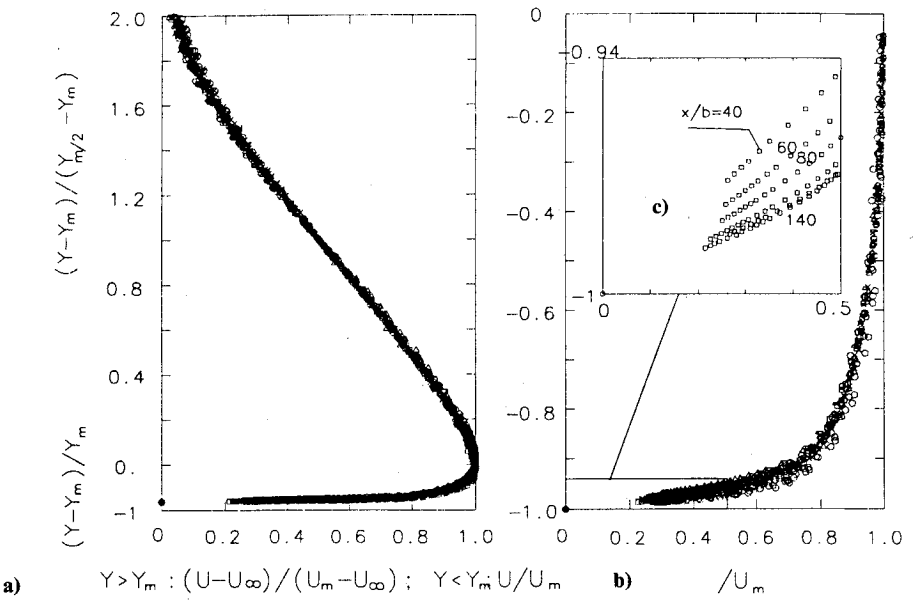

Fig. 5 Self-similarity of the normalized mean velocity profile.

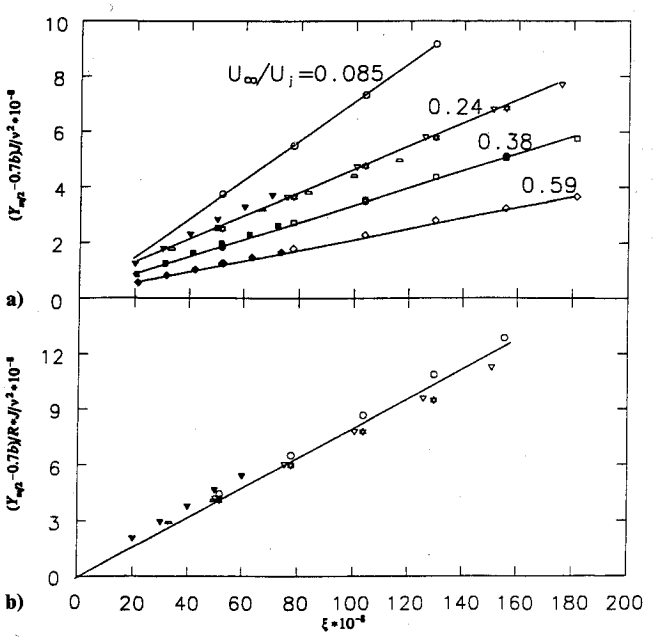

Fig. 6 Collapse of the rate of spread of the wall jet onto a single curve.

its similarity to the parameter scaling the spreading rate of a turbulent mixing layer between two parallel streams. We shall now define

$$\frac{U_m \nu R}{J} = F_1(\xi), \quad \frac{(Y_m - 0.2b)J}{\nu^2} = F_2(\xi), \quad \frac{U_0 \nu}{J} = F_3(\xi)$$

$$\frac{(Y_0 - 0.5b)J}{R\nu^2} = F_4(\xi), \quad \frac{(Y_{m/2} - 0.7b)J}{R\nu^2} = F_5(\xi)$$

$$\frac{\tau_w R}{\rho}\left(\frac{\nu}{J}\right)^2 = F_6(\xi) \tag{4}$$

where $Y_0 \equiv (Y_{m/2} - Y_m)$ and $U_0 \equiv (U_m - U_\infty)$.

The first four parameters scale the similarity profile plotted in Fig. 5. Some of these parameters depend on R, whereas others like Y_m clearly do not. It was also expected that the dependence of Y_0 on R will resemble the dependence of $Y_{m/2}$ on R since $Y_{m/2} \gg Y_m$ in the range of velocity ratios considered. Some of the interdependence of these parameters on R can be determined from the momentum integral equation that also exposes the limitations of the similarity approach when the range of an "approximate similarity" is limited to $U_\infty/U_j \ll 1$. Consequently, the utility of the momentum integral equation in calculating the skin friction[5] is much more limited in the present case.

The dependent parameters defined in Eq. (4) are plotted in Fig. 7. Other results, consistent with the limitation on $U_\infty/U_m \leq 0.5$ and collected from various articles,[5,7-10] are also plotted in Fig. 7 for comparison. The primary variables $Y_{m/2}$ and U_m were expressed by power laws that are in fair agreement with the exponents suggested for the wall jet in the absence of an external stream.[5] The scatter observed in these two quantities is not large even though the two cases in which the upstream boundary layer was artificially thickened are included in the figure (see Table 1). The outer velocity and length scales U_0 and Y_0 are more sensitive to the thickness of the upstream boundary layer that is mostly responsible for the reduction of the maximum velocity in the jet. This could be expected because the momentum loss in the upstream boundary layer was discarded in this analysis. A thick boundary layer causes the reduction in velocity above the jet near the nozzle (Fig. 2), therefore slowing down U_0. The inner and outer velocity and length scales vary with ξ at almost the same exponent, thus keeping the velocity profiles self-similar for a prescribed set of initial conditions. One should be careful to exclude from these correlations data points measured in the neighborhood of the slot where the wall jet is not fully developed.

The measured wall stress indicates a considerable amount of scatter at low Re_j and at small values of ξ. At higher values of ξ, the dependence of $F_6(\xi)$ may also be described by a power law. The skin friction is more sensitive to Reynolds number near the slot than any other quantity, partly because of transition. It is known that the skin friction during the last stages of transition or immediately following transition tends to be higher than in fully developed turbulent flow. Furthermore, τ_w is not inversely proportional to R as was assumed in Eq. (4). Its dependence on R, derived from the momentum integral equation, is rather complex as a consequence of the lack of self-similarity. The imposed restriction on $U_\infty/U_m \leq 0.5$ is more important in this case.

The following correlations may be used to predict the behavior of incompressible wall jets with and without a uniform

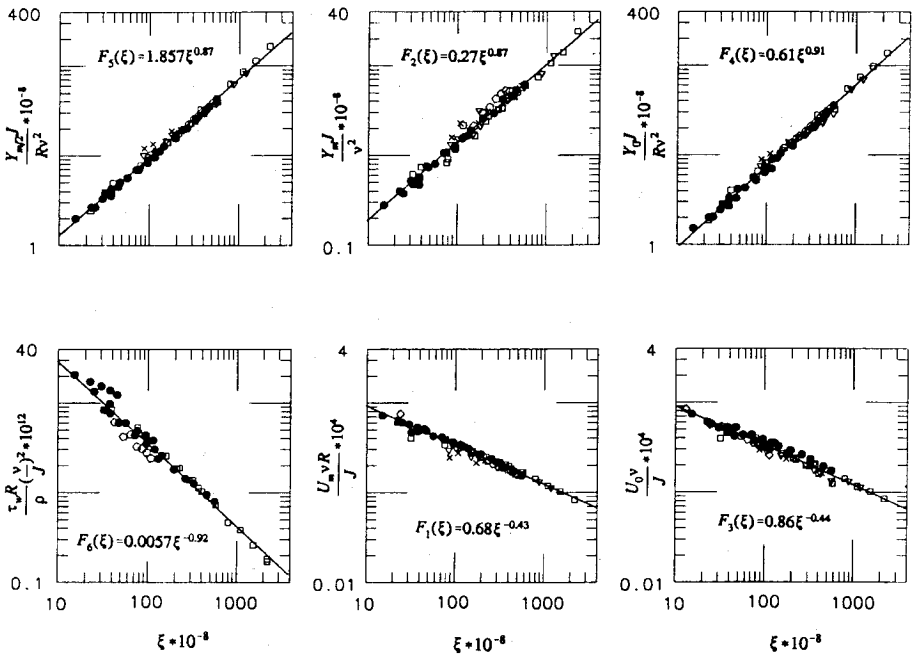

Fig. 7 Dependence of all velocity and length scales on ξ; present data and data from Refs. 5 and 7–10 are included: ● = present data, ⬠ = Ref. 5, × = Ref. 7, ⊡ = Ref. 8, ◇ = Ref. 9, and ▽ = Ref. 10.

external stream, provided the maximum velocity in the jet is at least twice as large as the freestream velocity:

$$\frac{Y_{m/2}J}{R\nu^2}=1.857(\xi)^{0.87},\quad \frac{Y_mJ}{\nu^2}=0.27(\xi)^{0.87},\quad \frac{Y_0J}{R\nu^2}=0.61(\xi)^{0.91}$$

$$\frac{\tau_wR}{\rho}\left(\frac{\nu}{J}\right)^2=0.0057(\xi)^{-0.92},\quad \frac{U_m\nu R}{J}=0.68(\xi)^{-0.43}$$

$$\frac{U_0\nu}{J}=0.86(\xi)^{-0.44} \tag{5}$$

These power laws should be practically independent of Re_j and θ_0. Only the wall shear stress τ_w measured in the absence of an external velocity appears to be somewhat lower.

Conclusions

One may extend the notion of self-similarity to a wall jet in a uniform stream provided $U_m/U_\infty \geq 2$. By doing so, all available data that characterize this flow collapsed onto a set of universal curves independent of Re and the thickness of the upstream boundary layer. This set of curves may be used in engineering applications.

Acknowledgment

The work was supported in part by a grant from the Air Force Office of Scientific Research, Contract AFOSR-88-0176, monitored by J. McMichael.

References

[1]Launder, B. E., and Rodi, W., "The Turbulent Wall Jets," *Progress in Aerospace Sciences,* Vol. 19, Pergamon, London, 1981, pp. 81–128.

[2]Launder, B. E., and Rodi, W., "The Turbulent Wall Jet—Measurements and Modeling," *Annual Reviews of Fluid Mechanics,* Vol. 15, 1983, pp. 429–459.

[3]Tailland, A., and Mathieu, J., "Jet Parietal," *Journal de Mecanique,* Vol. 6, No. 1, 1967, pp. 103–131.

[4]Narasimha, R., Narayan, K. Y., and Parthasarathy, S. P., "Parametric Analysis of Turbulent Wall Jets in Still Air," *Aeronautical Journal,* Vol. 77, July 1973, pp. 355–359.

[5]Wygnanski, I., Katz, Y., and Horev, E., "On the Applicability of Various Scaling Laws to the Turbulent Wall-Jet," *Journal of Fluid Mechanics,* Vol. 234, Jan. 1992, pp. 669–690.

[6]Irwin, H. P. A. H., "Measurements in a Self Preserving Plane Wall Jet in a Positive Pressure Gradient," *Journal of Fluid Mechanics,* Vol. 61, Oct. 1973, pp. 33–63.

[7]Patel, R. P., "Turbulent Jets and Wall Jets in Uniform Streaming Flow," *Aeronautical Quarterly,* Vol. 22, Nov. 1971, pp. 311–326.

[8]Kruka, V., and Eskinazi, S., "The Wall-Jet in a Moving Stream," *Journal of Fluid Mechanics,* Vol. 20, Dec. 1964, pp. 555–579.

[9]Seban, R. A., and Back, L. H., "Velocity and Temperature Profiles in a Wall Jet," *International Journal of Heat and Mass Transfer,* Vol. 3, Dec. 1961, pp. 255–265.

[10]Gartshore, I. S., and Newman, B. G., "The Turbulent Wall Jet in an Arbitrary Pressure Gradient," *Aeronautical Quarterly,* Vol. 20, Feb. 1969, pp. 25–56.